

# Plasmonic enhancement of a whispering-gallery-mode biosensor for single nanoparticle detection

S. I. Shopova,<sup>1,a)</sup> R. Rajmangal,<sup>1</sup> S. Holler,<sup>1,2</sup> and S. Arnold<sup>1</sup>

<sup>1</sup>*Microparticle Photophysics Lab, Polytechnic Institute of NYU, Brooklyn, New York 11201, USA*

<sup>2</sup>*Thermo Fisher Scientific, Redwood Shores, California 94065, USA*

(Received 31 March 2011; accepted 15 May 2011; published online 13 June 2011)

We describe and demonstrate a physical mechanism that substantially enhances the label-free sensitivity of a whispering-gallery-mode biosensor for the detection of individual nanoparticles in aqueous solution. It involves the interaction of dielectric nanoparticle in an equatorial carousel orbit with a plasmonic nanoparticle bound at the microparticle's equator. As the dielectric particle parks to hot spots on the plasmonic particle we observe frequency shifts that are enhanced by a factor of 4, consistent with a simple reactive model. Once optimized the enhancement by this mechanism should exceed several orders of magnitude, putting individual protein within reach. © 2011 American Institute of Physics. [doi:10.1063/1.3599584]

The need for fast and early detection of pathogens (e.g., virus) and the antibodies that are generated as a biological response has led to the invention of ultrasensitive label-free whispering gallery mode (WGM) biosensors that can detect individual bionanoparticles in aqueous solution.<sup>1</sup> Following the initial theory indicating that these WGM devices should be sensitive to a single virion in water,<sup>2,3</sup> the goal was recently fulfilled with the detection of Influenza A on a microspherical silica resonator.<sup>4</sup> The idea leading to this achievement was that a nanoparticle entering the WGM's evanescent field causes the mode to shift its frequency in reaction to being polarized by the field.<sup>2</sup> The fractional shift in frequency  $\Delta\omega_r/\omega_r$  is the negative of the energy required to polarize the particle,  $|W_p|$ , over that of the medium divided by the energy in the cavity  $W_c$ ;  $\Delta\omega_r/\omega_r = -|W_p|/W_c$ . This simple rule, known as the reactive sensing principle (RSP), has been shown to apply so long as the linewidth of the mode  $\delta\omega_r$  is considerably larger than the shift  $\Delta\omega_r$  (Refs. 4–6). For a Rayleigh particle the RSP for the fractional frequency shift and the fractional shift in the free-space wavelength tracking the mode,  $\Delta\lambda_r/\lambda_r$ , are<sup>2</sup>

$$\frac{\Delta\omega_r}{\omega_r} = -\frac{\Delta\lambda_r}{\lambda_r} = -\frac{|W_p|}{W_c} \cong -\frac{\alpha_{ex}|E_0(\mathbf{r}_v)|^2}{2\int\epsilon_c|E_0(\mathbf{r})|^2dV}, \quad (1)$$

where  $\alpha_{ex}$  is the excess polarizability of the nanoparticle,  $\epsilon_c$  is the permittivity of the cavity, and  $E_0(\mathbf{r}_v)$  and  $E_0(\mathbf{r})$  are modal field amplitudes at the position of the nanoparticle  $\mathbf{r}_v$  and throughout the mode, respectively. Since the energy required to polarize a nanoparticle is proportional to its polarizability  $\alpha_{ex}$ , the frequency shift is proportional to its mass  $m$ . At present, noise and mode volume limitations of a microspherical silica resonator have set the limit of detection (LOD) in water to  $m_{\text{LOD}} \sim 20$  ag (radius  $a_{\text{LOD}} \sim 17$  nm).<sup>5</sup> To definitively detect single protein requires considerably better sensitivity ( $m_{\text{protein}} \sim 0.1$  ag). In what follows we outline an enhancement mechanism that can accomplish this goal.

This mechanism involves creating local plasmonic “hot spots” near the sensing equator within the WGM's evanescent field. Plasmonic nanoparticles grown on the surface of a WGM resonator have been shown to locally enhance the evanescent field without significantly degrading the  $Q$ .<sup>7</sup> In the current letter a controlled deposition was accomplished by guiding a plasmonic nanoparticle to the microsphere's equator using carousel forces,<sup>6</sup> where it is seen to bind (most

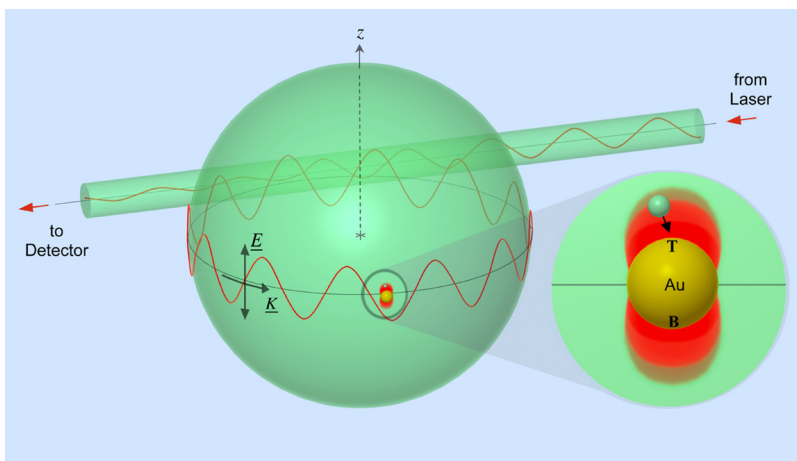


FIG. 1. (Color online) Illustrates a traveling WGM interacting with a stationary gold nanoparticle stimulated into a plasmonically resonant dipole mode. This generates hot spots north and south of the equator that capture smaller dielectric nanoparticles as the WGM's Carousel forces are transporting them. The effect is an enhanced resonant shift of the microcavity's frequency.

<sup>a)</sup>Author to whom correspondence should be addressed. Electronic mail: sshopova@poly.edu.

likely to a defect site<sup>8</sup>) as in Fig. 1. To estimate the enhancement we suppose that the WGM is the lowest order transverse electric (TE) mode with an approximately Gaussian shaped intensity profile having a breadth of a few microns around the equator, thereby bathing the plasmonic nanoparticle in a nearly uniform field. Excitation of the dipole resonance of this particle with modal field amplitude  $E_0$  generates hot spots in intensity as seen in Fig. 1. Enhanced gradient forces capture a dielectric nanoparticle at one of these spots.<sup>9,10</sup> Since the hot spots are part of the local field of the plasmonically modified microresonator, the resonance frequency undergoes an enhanced shift by comparison with binding to the bare resonator. Based on the RSP the enhancement  $R_E$  is produced by the relative increase in polarization energy of an analyte particle at a hot spot in comparison to that in the absence of the plasmonic particle. If we suppose that an extremely small particle of radius  $a_d$  (e.g., protein) is drawn to the top (T, Fig. 1) of the plasmonic particle of radius  $a_p$  the enhancement can be written as

$$R_{E,\max} \approx \left| 1 + 2 \left( \frac{1}{1 + a_d/a_p} \right)^3 \left( \frac{\varepsilon_p - \varepsilon_m}{\varepsilon_p + 2\varepsilon_m} \right) \right|^2, \quad (2)$$

where  $\varepsilon_p$  and  $\varepsilon_m$  are the relative permittivity of the metal (e.g., gold or silver) and medium (i.e., water). In arriving at Eq. (2) we have assumed that the target dielectric nanoparticle is considerably smaller than the metallic nanoparticle so that spatial variations in the field within it can be ignored, and that both are close enough to the resonator surface in order to avoid including the slight fall off in the evanescent intensity between the microsphere surface and the nanoparticle centers. We also assumed that the binding potential between the image dipole in the metal and the induced dipole in the dielectric particle is not significant. To gain an estimate for the effect associated with parking a protein on a homogeneous plasmonic particle, we will take  $a_d/a_p \approx 0$ . If now  $\varepsilon_p = \varepsilon_m$ , the enhancement disappears (i.e.,  $R_E = 1$ ), and for a perfect metal for which  $\varepsilon_p$  has an infinite magnitude  $R_E = 9$ , both of which are reasonable results.<sup>11</sup> More interestingly, at the dipole plasmonic resonance frequency  $\omega_1$ , where the real part of the of the metallic permittivity is controlled by the medium [i.e.,  $\text{Re}[\varepsilon_p(\omega_1)] = -2\varepsilon_m = -3.5$  for water] the enhancement is limited principally by the  $\text{Im}[\varepsilon_p(\omega_1)]$ . For a gold nanoparticle in water<sup>12</sup> at resonance  $\text{Im}[\varepsilon_{pg}(\omega_1)] \approx 2$ , which gives an enhancement  $R_{Eg} \approx 37$ . The enhancement should be substantially greater for silver because  $\text{Im}[\varepsilon_{ps}(\omega_1)]$  is considerably smaller than in gold (0.7 versus 2); we estimate the enhancement for a silver nanoparticle to be 234.

Our experiments are aimed at comparing frequency shifts of particles landing on a bare silica surface with shifts for particles parking on a bound plasmonic nanoparticle. A typical experiment showing distinct enhancement is described next. In order to establish a benchmark we used dielectric nanoparticles with radii a lot larger than protein (55 nm versus 3 nm). Our WGM resonator is a fused silica microsphere ( $R = 33.5 \pm 0.5 \mu\text{m}$ ) prepared by heating the end of a tapered optical fiber in a focused beam of  $\text{CO}_2$  laser. The optimal frequency shift of a bare silica microsphere occurs when a nanoparticle is deposited at the equator, where the WGM field is greatest. For an equatorial TE WGM of this microspherical resonator the RSP [Eq. (1)] has been evaluated<sup>4-6</sup> for a nanoparticle binding to the equator and predicts a wavelength shift of 25 fm for a 55 nm polystyrene

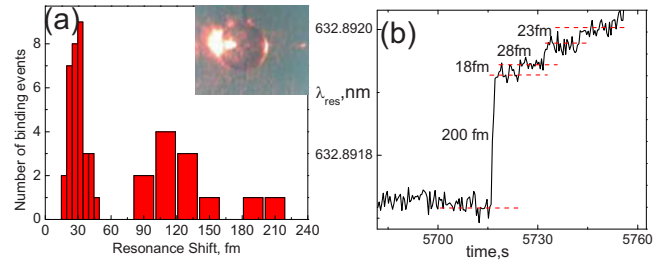


FIG. 2. (Color online) (a) Shift statistics after injecting PS particles into a cell with a WGM resonator having gold nanoshells bound to its equator; inset: a typical image showing scattering from a Au shell on the surface (b) wavelength shift data showing steps from the two groups.

(PS) particle. To test for enhancement, we functionalized the equator of a microsphere with gold nanoshells (Nanospectra Biosciences Inc. lot No. NS20080116, nominal outer radius of 70 nm) and monitored the resonator response in the presence of dielectric nanoparticles. As we will show a number of events substantially exceeded the benchmark set by RSP.

The resonator is immersed in de-ionized (DI) water and enclosed in a microfluidic cell. The sphere is brought in contact with a tapered optical fiber, transmitting 632.8 nm light from a tunable external cavity laser source to evanescently excite a WGM. This laser is tuned to a resonance of the microsphere having a  $Q$  of  $5 \times 10^5$ . Gold nanoshells were injected into the 100  $\mu\text{L}$  microfluidic cell at a concentration of  $\sim 10^6$  particles/mL. At our excitation wavelength the average nanoshell is excited into a quadrupole/dipole superposition based on the extinction spectrum of the hydrosol. As in carousel force experiments<sup>6</sup> we observed a few particles drawn to the equator of the resonator by evanescent gradient forces. After visual observation of light scattering revealed three binding events, the laser was turned off and the microfluidic cell was rinsed with DI water for  $\sim 2$  min to eliminate all unbound gold nanoshells from solution. With the laser light restored previously bound gold nanoshells appeared to remain at the same locations on the surface. The cell was then filled with phosphate buffered saline solution (PBS) and left for 5 min to establish a zero accumulation signal. A PBS dispersion of PS nanospheres with nominal radius of 55 nm as measured by dynamic light scattering was then added at a concentration of 60 fM. The adsorption of PS nanoparticles on the plasmonically modified microsphere surface results in multiple steps of the resonant wavelength that clearly separate into two groups as shown in the histogram in Fig. 2(a). The first group consists of steps with a wavelength shift having a most probable value at 30 fm consistent with the shift obtained from RSP (30 fm) using the mean radius reported by the manufacturer (60 nm, Polysciences). The second group consists of considerably larger wavelength shift steps (up to 216 fm). This represents an  $\sim 4 \times$  enhancement from the largest wavelength shift in the first group (47 fm). The breadth of each of the groups is attributed to the size distribution of the particles, and slight variations in their binding locations. Figure 2(b) shows a typical example of the binding data that includes a giant step associated with the second region along with smaller steps associated with the first (see Ref. 13).

To understand the second group requires that we simulate the local intensity that would be seen by the dielectric particles as they park on plasmonic hot spots. At the wavelength used, a gold nanoshell of nominal size would be pri-

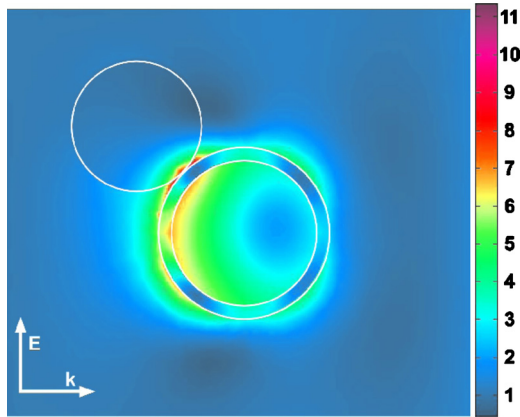


FIG. 3. (Color online) FEM simulation of the parking of 55 nm radius PS sphere at one of the forward quadrupole lobes of a plasmonic nanoshell with 60 nm inner core radius of SiO<sub>2</sub> and 10 nm shell thickness of Au. The field amplitude at the point of contact grows to just over 11× the field of the 633 nm TE mode as indicated by the rainbow scale on the right.

marily excited into a quadrupole mode, as shown in the finite element method (FEM) simulation in Fig. 3. The four lobes of this field have intensities that drop off very rapidly. We also show a parking place for the 55 nm radius dielectric sphere leading to optimal field overlap.

Now the major question is: how large is the influence on the WGM of a plasmonically parked dielectric particle in comparison with the same particle that binds directly to the silica surface? This can be answered by calculating the ratio of the excess polarization energy of the dielectric particle at a plasmonic hot spot to that at the silica surface in the presence of the same WGM. Because the quadrupole lobe penetrates into a small portion of the nanoparticle, we cannot use a simple dipole approximation as we did on the silica surface. Instead we will represent the excess polarization energy in each case more generally by numerically integrating  $\Delta\epsilon \mathbf{E}_b \cdot \mathbf{E}_a^*$  over the nanoparticle's volume,<sup>14</sup> where  $\Delta\epsilon = \epsilon_d - \epsilon_m$  with  $\epsilon_d$  being the relative permittivity of the dielectric particles and  $\mathbf{E}_b \cdot \mathbf{E}_a^*$  is the product of the field before the particle insertion with that after the particle insertion. We have computed this integral using FEM simulation and found that the ratio of the integral evaluated for the particle binding as in Fig. 3 to that for direct binding to the microcavity's equator is 3.1 in good agreement with the experimentally estimated enhancement of  $\sim 4$ .

One clear characteristic of Fig. 3 is that the penetration depth of the field into the dielectric particle from the gold nanoshells is far smaller than the particle's radius, causing the enhancement to be massively reduced; only the small sliver of material near the contact interface is significantly polarized. Consequently as particle sizes are reduced to the size of a MS2 virus ( $a_d \approx 12$  nm) the enhancement should

grow, and indeed it does. By using the same FEM approach for the MS2 virus positioned on a quadrupole lobe as in Fig. 3, we compute an enhancement of 16.5 at the quadrupole resonance (649 nm). Still the field is found to be only partially penetrating. If we extend our simulation to a single protein such as bovine serum albumin (BSA,  $a_d \approx 3$  nm), the enhancement grows to 37.3. Greater enhancements are expected at a dipole resonance. For the same nanoshells as in Fig. 3 the dipole should be reached at 810 nm and produce an intensity pattern similar to that in Fig. 1 (i.e., two lobes). Since the dipole near field falls off much more slowly than the quadrupole field, overlap between the field and the particle's dielectric form is improved. The net effect is that the enhancement for an MS2 virus falling into a dipole lobe is 101.0. For BSA the theoretical enhancement is even higher at 199.0.

Recently, the LOD for biodetection by WGM devices has been reduced to an equivalent radius of  $\sim 17$  nm, by using an ultralow noise laser source for a microsphere having  $Q \sim 10^6$ .<sup>5</sup> An enhancement of 199 in the wavelength shift is expected to reduce the detectable radius to  $\sim 17$  nm/(199)<sup>1/3</sup> or 2.9 nm, which clearly is below the size of the smallest virus and in the range of an intermediate sized protein. This projection implies that plasmon-WGM hybrid resonators may be an answer to label-free single molecule (i.e., protein) detection in the future.

The authors thank the NSF for supporting this work (Grant No. CBET 0933531). We are also grateful to William Chin of the MP<sup>3</sup>L for preparing Fig. 1.

<sup>1</sup>Y. Sun and X. D. Fan, *Anal. Bioanal. Chem.* **399**, 205 (2011).

<sup>2</sup>S. Arnold, M. Khoshshima, I. Teraoka, S. Holler, and F. Vollmer, *Opt. Lett.* **28**, 272 (2003).

<sup>3</sup>S. Arnold, R. Ramjit, D. Keng, V. Kolchenko, and I. Teraoka, *Faraday Discuss.* **137**, 65 (2008).

<sup>4</sup>F. Vollmer, S. Arnold, and D. Keng, *Proc. Natl. Acad. Sci. U.S.A.* **105**, 20701 (2008).

<sup>5</sup>S. I. Shopova, R. Rajmangal, Y. Nishida, and S. Arnold, *Rev. Sci. Instrum.* **81**, 103110 (2010).

<sup>6</sup>S. Arnold, D. Keng, S. I. Shopova, S. Holler, W. Zurawsky, and F. Vollmer, *Opt. Express* **17**, 6230 (2009).

<sup>7</sup>S. I. Shopova, C. W. Blackledge, and A. T. Rosenberger, *Appl. Phys. B: Lasers Opt.* **93**, 183 (2008).

<sup>8</sup>U. Martinez, J. Jerratsch, L. Niklas, N. Giordano, G. Pacchioni, and H.-J. Freund, *Phys. Rev. Lett.* **103**, 056801 (2009).

<sup>9</sup>A. Ashkin, J. M. Dziedzic, J. E. Bjorkholm, and S. Chu, *Opt. Lett.* **11**, 288 (1986).

<sup>10</sup>L. Novotny, R. X. Bian, and X. S. Xie, *Phys. Rev. Lett.* **79**, 645 (1997).

<sup>11</sup>J. R. Reitz, F. J. Milford, and R. W. Christy, *Foundations of Electromagnetic Theory*, 3rd ed. (Addison-Wesley, Reading, MA, 1980).

<sup>12</sup>P. Stoller, V. Jacobsen, and V. Sandoghdar, *Opt. Lett.* **31**, 2474 (2006).

<sup>13</sup>See supplementary material at <http://dx.doi.org/10.1063/1.3599584> for an extended trace of the resonant shift in time showing the frequency of binding events.

<sup>14</sup>J. D. Jackson, *Classical Electrodynamics*, 3rd ed. (Wiley, Hoboken, NJ, 1999).